RAPID MACROCELL TESTS OF LDX 2101® STAINLESS STEEL BARS

By
Matthew O'Reilly
W. Joseph Sturgeon
David Darwin
JoAnn Browning

A Report on Research Sponsored by

OUTOKUMPU STAINLESS – NORTH AMERICA

Structural Engineering and Engineering Materials
SL Report 10-2
May 2010

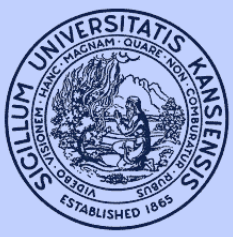

THE UNIVERSITY OF KANSAS CENTER FOR RESEARCH, INC.
2385 Irving Hill Road, Lawrence, Kansas 66045-7563

RAPID MACROCELL TESTS OF LDX 2101® STAINLESS STEEL BARS

By

Matthew O'Reilly

W. Joseph Sturgeon

David Darwin

JoAnn Browning

Research supported by

OUTOKUMPU STAINLESS – NORTH AMERICA

Structural Engineering and Engineering Materials
SL Report 10-2

THE UNIVERSITY OF KANSAS CENTER FOR RESEARCH, INC.
LAWRENCE, KANSAS
May 2010

ABSTRACT

The corrosion resistance of LDX 2101® duplex stainless steel bars is evaluated using the rapid macrocell test specified in Annex A2 of ASTM A955-09b and compared to the performance of 2205 pickled stainless steel (2205p). LDX 2101® bars were tested in the as-received condition as well as after submersion in simulated concrete pore solution with a pH of 13.4 for two weeks prior to testing.

The LDX 2101® stainless steel bars meet the requirements of ASTM A955-09b, exhibiting limited staining and slight corrosion on the bars in salt solution with a maximum individual corrosion rate of 0.44 μm/yr and a maximum average corrosion rate of 0.10 μm/yr. No significant difference was observed in the behavior between bars tested in the as-received condition and bars tested after submersion in simulated concrete pore solution. The 2205p bars exhibited no visible corrosion products on the bars in salt solution and no measureable corrosion. Both the LDX 2101® and 2205p stainless steel bars exhibited moderate staining of the bars used as cathodes in oxygenated pore solution.

Keywords: chlorides, concrete, corrosion, macrocell, reinforcing steel, stainless steel

ACKNOWLEDGEMENTS

The research described in this report was supported by Outokumpu Stainless – North America. The 2205 stainless steel used in this study was provided by Gerdau AmeriSteel.

INTRODUCTION

This report describes the tests used to evaluate the corrosion performance of LDX 2101® stainless steel bars. Performance is compared to that of pickled 2205 stainless steel.

EXPERIMENTAL WORK

Materials

Tests were performed on No. 6 (No. 19) LDX 2101® stainless steel bars. The bars were inspected upon receipt and found to be in good condition with the exception of wear on the bars from tie-down straps used in shipping (Figure 1) and isolated defects to the surface (Figure 2). Sections of bar affected by the wear or damage were not used in testing.

The deformation pattern on the bars is noted in Figures 1 and 2. The pattern features a taper on the transverse deformations and three equally spaced longitudinal ribs. Two longitudinal ribs are currently standard for bars meeting the provisions of ASTM A955-09b.

Figure 1: Damage to stainless steel sustained during shipping.

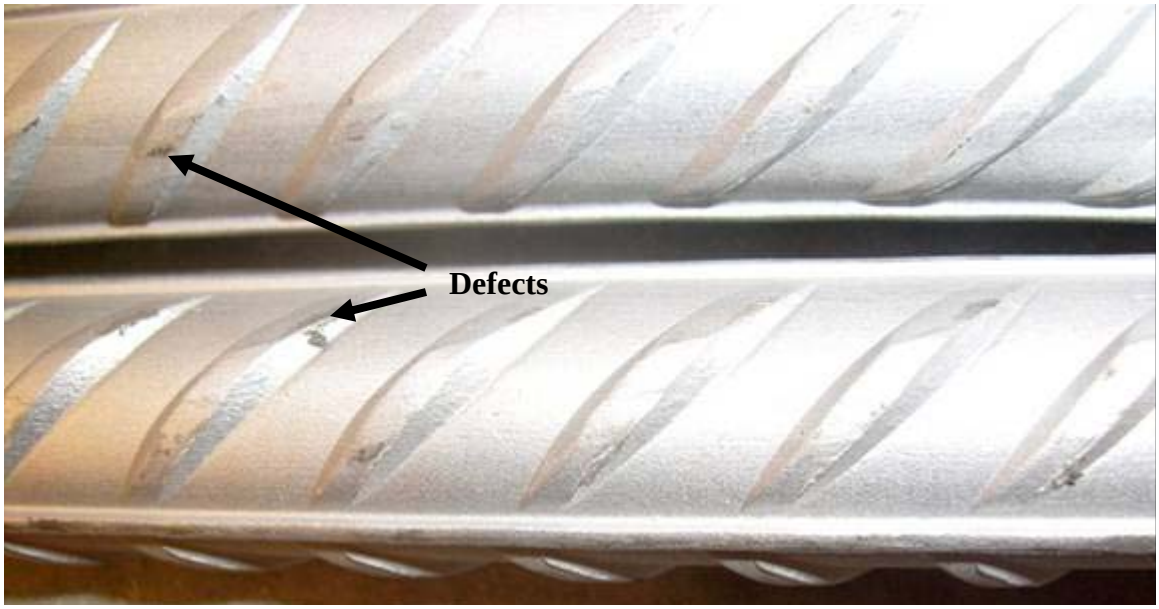

Figure 2: Surface defects in stainless steel.

According to the supplier, the LDX 2101® bars underwent a two-cycle cleaning and pickling procedure. Each cycle consisted of shot-blasting to remove surface scale followed by pickling for one hour at 140° F in a mix of nitric acid and hydrofluoric acid, followed by a water rinse. The 2205p bars were blasted to a near white condition with stainless grit and pickled in a 25% nitric acid, 3-6% hydrofluoric acid solution at 110° F for 40-50 minutes.

The chemical compositions of the two stainless steels are given in Tables 2a and 2b.

Table 2a: Chemical Compositions of Stainless Steels (Provided by Manufacturers)

Material	Cr	Ni	C	Mn	N	P	S	Mo	Si	Sn	Cu	Nb
LDX 2101®	21.58	1.49	0.035	4.81	0.231	0.024	0.001	0.14	0.712	0.010	0.306	0.015
2205p	22.27	4.88	0.020	1.37	0.192	0.023	0.001	3.26	0.420	-	0.300	-

Table 2b: Chemical Compositions of Stainless Steels (Continued)

Material	W	V	Co	Ti	As	B	Pb	Ca	Ta
LDX 2101®	0.050	0.150	0.051	0.006	0.011	0.0019	0.0001	0.0032	0.005
2205p	-	-	-	-	-	-	-	-	-

Experimental Procedures

Rapid Macrocell Test

A total of 15 specimens were tested in accordance with the rapid macrocell corrosion test outlined in Annex A2 of ASTM A955-09b and pictured in Figure 3. Each bar used in the rapid macrocell is 5 in. long and is drilled and tapped at one end to accept a 0.5-in. 10-24 stainless steel machine screw. Bars are cleaned with acetone to remove surface oil and contaminants introduced by machining. A length of 16-gauge insulated copper wire is attached to each bar via the machine screw. The electrical connection is coated with an epoxy to protect the wire from corrosion.

A single rapid macrocell specimen consists of an anode and a cathode. The cathode consists of two bars submerged in simulated pore solution in a plastic container, as shown in Figure 3. One liter of pore solution consists of 974.8 g of distilled water, 18.81 g of potassium hydroxide (KOH), and 17.87 g of sodium hydroxide (NaOH). The solution has a pH of about 13.4. Air, scrubbed to remove carbon dioxide, is bubbled into the cathode solution. The anode consists of a single bar submerged in a solution consisting of simulated pore solution and 15 percent sodium chloride (NaCl). The “salt” solution is prepared by adding 172.1 g of NaCl to one liter of pore solution. The solutions are changed every five weeks to limit the effects of carbonation. The anode and cathode are connected electrically across a 10-ohm resistor. A

potassium chloride salt bridge provides an ionic connection between the anode and the cathode (Figure 3).

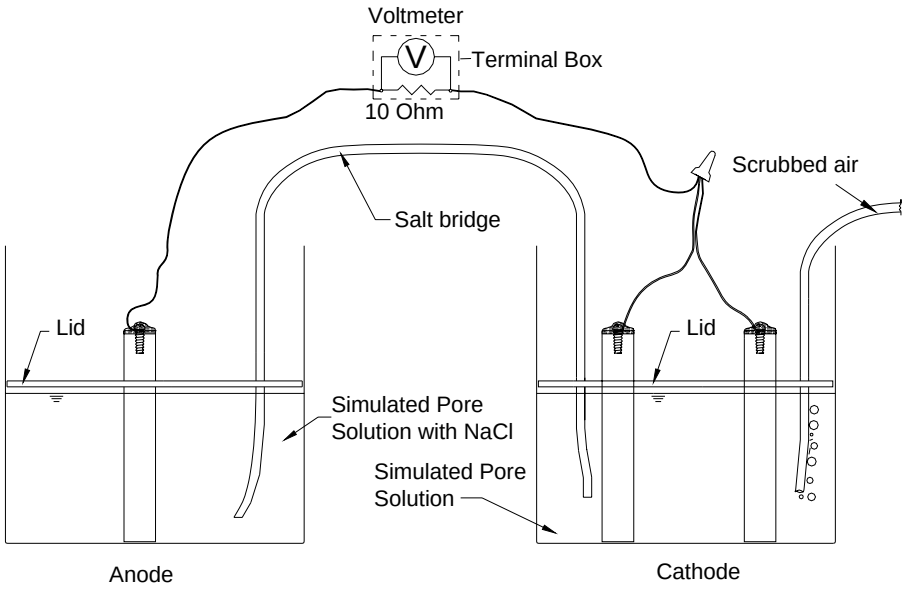

Figure 3: Rapid Macrocell Test Setup

ASTM A955-09b calls for No. 5 (No. 16) bars submerged to a depth of 3 in. Because No. 6 (No. 19) bars were provided, the depth of submersion was reduced to 2.44 in. to maintain the same exposed area of metal (end and sides) as obtained with No. 5 (No. 16) bars submerged to a depth of 3 in.

The corrosion rate is calculated based on the voltage drop across the 10-ohm resistor using Faraday's equation.

$$\text{Rate} = K \frac{V \cdot m}{n \cdot F \cdot D \cdot R \cdot A} \tag{2}$$

where the Rate is given in μm/yr, and

K = conversion factor = $31.5 \cdot 10^4$ amp·μm ·sec/μA·cm·yr

V = measured voltage drop across resistor, millivolts

m = atomic weight of the metal (for iron, m = 55.8 g/g-atom)

n = number of ion equivalents exchanged (for iron, n = 2 equivalents)

F = Faraday's constant = 96485 coulombs/equivalent

D = density of the metal, g/cm^3 (for iron, D = 7.87 g/cm^3)

R = resistance of resistor, ohms = 10 ohms for the test

A = surface area of anode exposed to solution, 39.9 cm^2

Using the values listed above, the corrosion rate simplifies to:

$$\text{Rate} = 29.0V \tag{3}$$

To satisfy ASTM A955-09b, no individual reading may exceed 0.50 μm/yr and the average rate of all specimens may not exceed 0.25 μm/yr. In both cases, the corrosion current must be such as to indicate net corrosion at the anode. Current indicating a "negative" value of corrosion, independent of value, does not indicate corrosion of the anode and is caused by minor differences in oxidation rate between the single anode bar and the two cathode bars.

In addition to the corrosion rate, the corrosion potential is measured at the anode and cathode using a saturated calomel electrode (SCE). Readings are taken daily for the first week and weekly thereafter.

A total of 12 LDX 2101® stainless steel specimens were tested. Nine were tested in the as-received condition but avoiding sections of bar with visible damage. Testing on specimens 7-9 began two weeks after starting testing on specimens 1-6. The remaining three specimens were completely submerged in pore solution for two weeks prior to the start of testing to simulate exposure to concrete prior to contact with chlorides. In addition, three specimens containing 2205 pickled stainless steel (2205p) were tested to serve as a comparison sample.

RESULTS

Individual corrosion rate data for the nine specimens tested in the as-received condition are shown in Figure 4 (Specimens 1-6) and Figure 5 (Specimens 7-9). Average corrosion rate data for all nine specimens is shown in Figure 6. As shown in the figures, the predominant corrosion rate is "negative," which, as explained before, is caused by minor differences in oxidation rate between the single anode bar and the two cathode bars. Figure 4 shows that specimen 3 exhibited a positive corrosion rate of 2.24 μm/yr at week 5, before the solution was changed. Immediately after the solution change, however, the corrosion rate fell to 0.44 μm/yr. It is believed that the single high corrosion rate data point is a statistical outlier or erroneous reading and is not sufficient reason to fail the stainless steel. No other specimen exceeded the 0.50 μm/yr limit during the course of the test. Excluding the Week 5 reading for specimen 3, individual corrosion rates ranged from −1.68 μm/yr to +0.38 μm/yr. As shown in Figure 6, the average corrosion rate ranged from −0.32 μm/yr to +0.10 μm/yr and was positive at week 5 and during weeks 14 and 15, never exceeding the +0.25 μm/yr limit (Figure 6).

During the tests, the bars in pore solution without salt (cathode bars) exhibited staining, possibly due to a reaction in the oxygenated cathodic environment. Although this behavior was observed for most specimens, it is not indicative of a susceptibility to corrosion in a chloride-contaminated concrete environment.

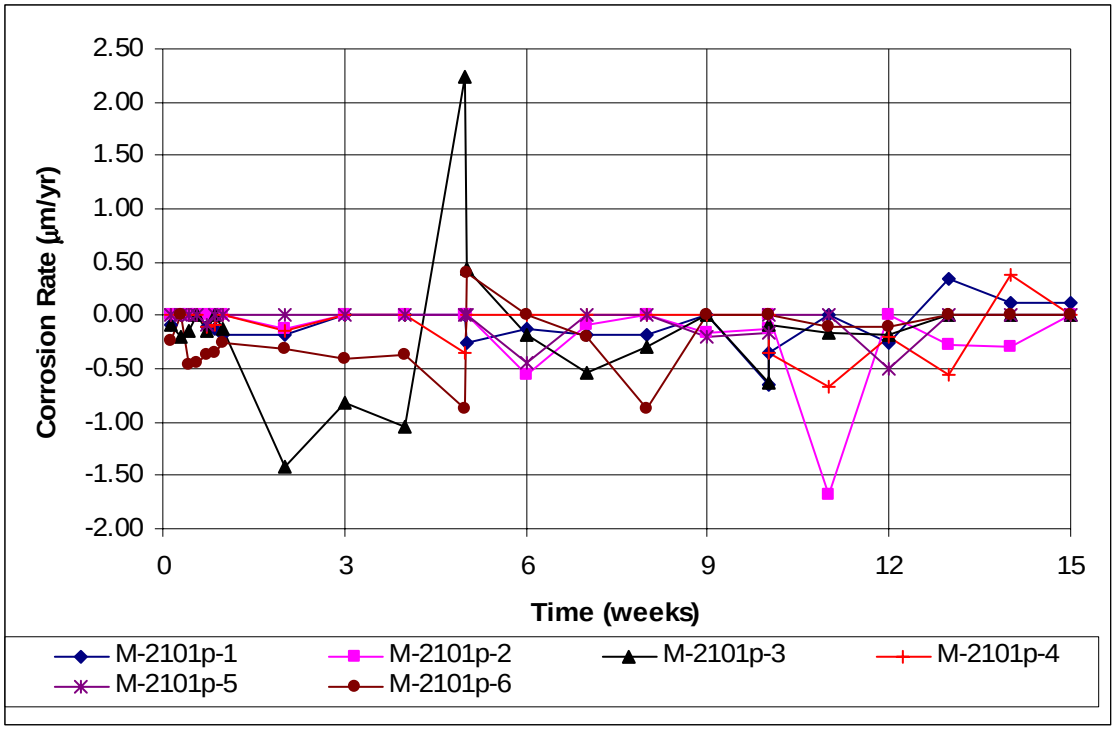

Figure 4: Individual corrosion rate. LDX 2101® specimens 1-6, as received condition.

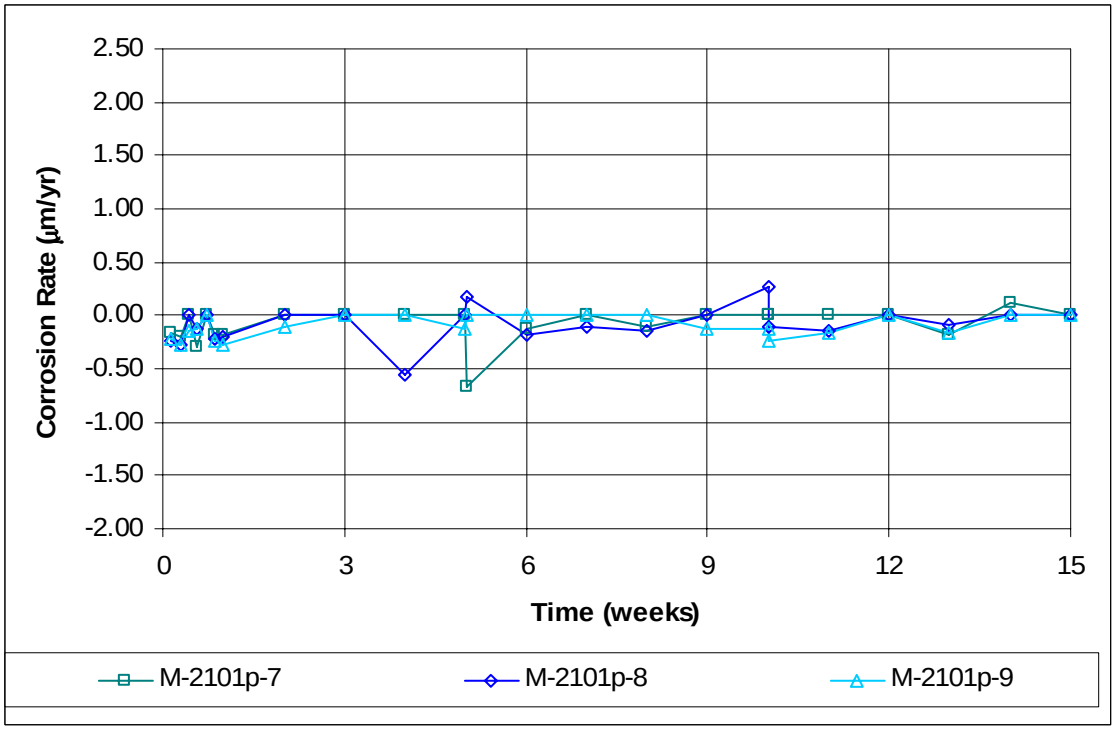

Figure 5: Individual corrosion rate. LDX 2101® specimens 7-9, as received condition.

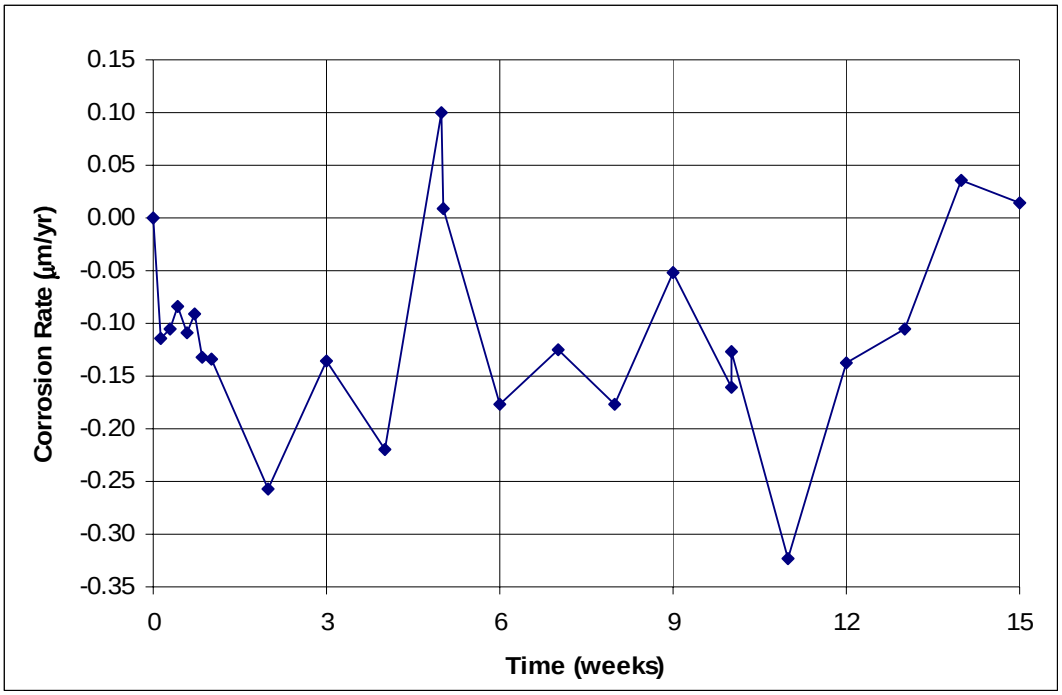

Figure 6: Average corrosion rate. LDX 2101® specimens 1-9, as received condition

Individual corrosion potentials with respect to a saturated calomel electrode are shown in Figures 7 and 8 for the bars in salt and pore solutions respectively. As seen in Figures 7 and 8, bars in salt solution and bars in pore solution exhibit corrosion potentials in the range of −0.100 V to −0.250 V with respect to a saturated calomel electrode. ASTM C876 states a corrosion potential more negative than -0.275 V with respect to a saturated calomel electrode (−0.350 V with respect to a copper/copper sulfate electrode) represents a greater than 90% probability of corrosion in concrete. Although all specimens exhibited corrosion potentials more positive than

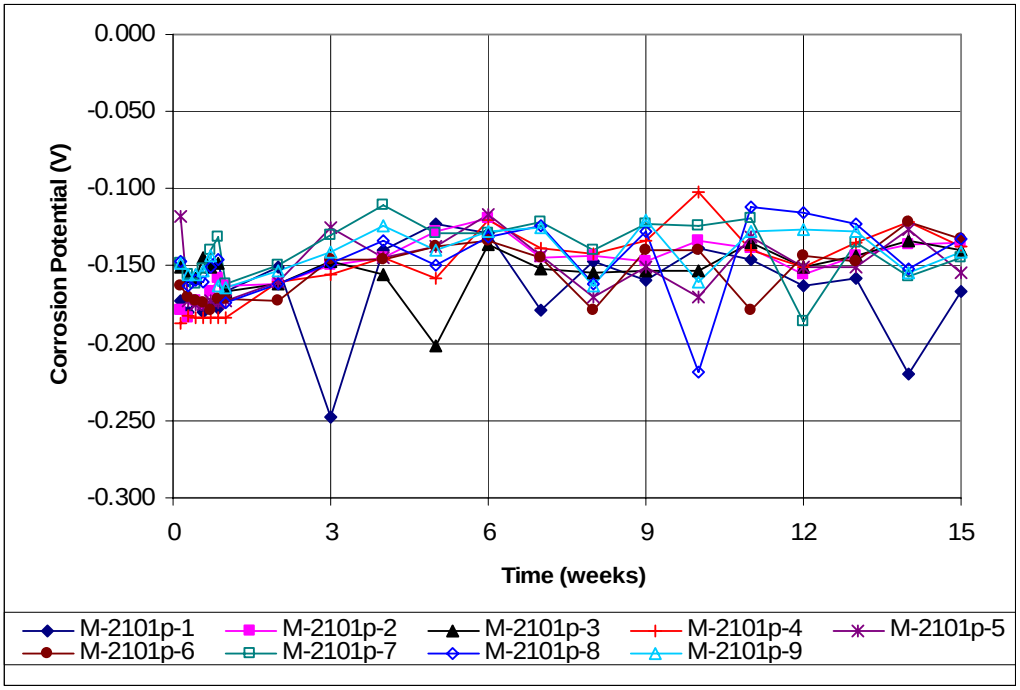

Figure 7: Individual corrosion potential with respect to SCE. Bars in salt solution (anode). LDX 2101® specimens 1-9, as received condition.

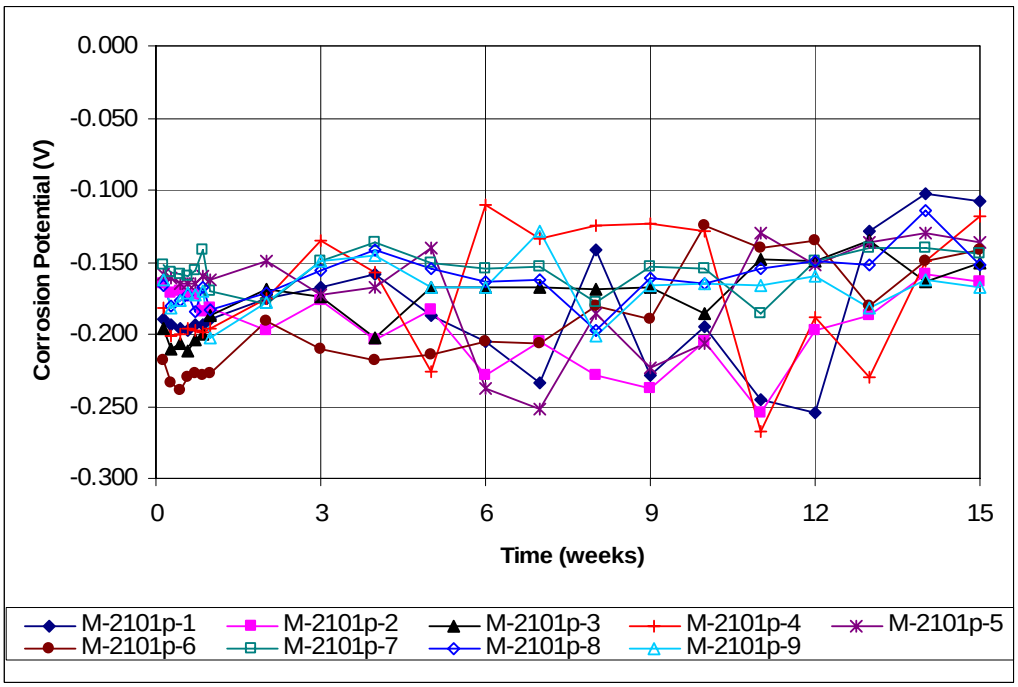

Figure 8: Individual corrosion potential with respect to SCE. Bars in pore solution (cathode). LDX 2101® specimens 1-9, as received condition.

−0.275 V, the tests are conducted in simulated pore solution and a direct comparison to C876 cannot be made. Potentials for bars in the pore solution were on average 40 mV more negative than bars in salt solution, as would be expected based on the "negative" corrosion rate observed in Figures 4-6.

Individual and average corrosion rate data for the three specimens submerged in simulated pore solution prior to testing are shown in Figures 9 and 10, respectively. Individual corrosion rates ranged from −0.83 µm/yr to +0.34 µm/yr. As shown in Figure 10, the average corrosion rate ranged from −0.44 µm/yr to +0.06 µm/yr and was positive at day 4 and week 6. Individual specimens exhibited positive corrosion rates at various points throughout the test (Figure 9), but at no point were the limits specified by Annex A2 of ASTM A955-09b exceeded. Overall, the performance of the specimens submerged in simulated pore solution prior to testing was similar to that of the bars tested in the as-received condition.

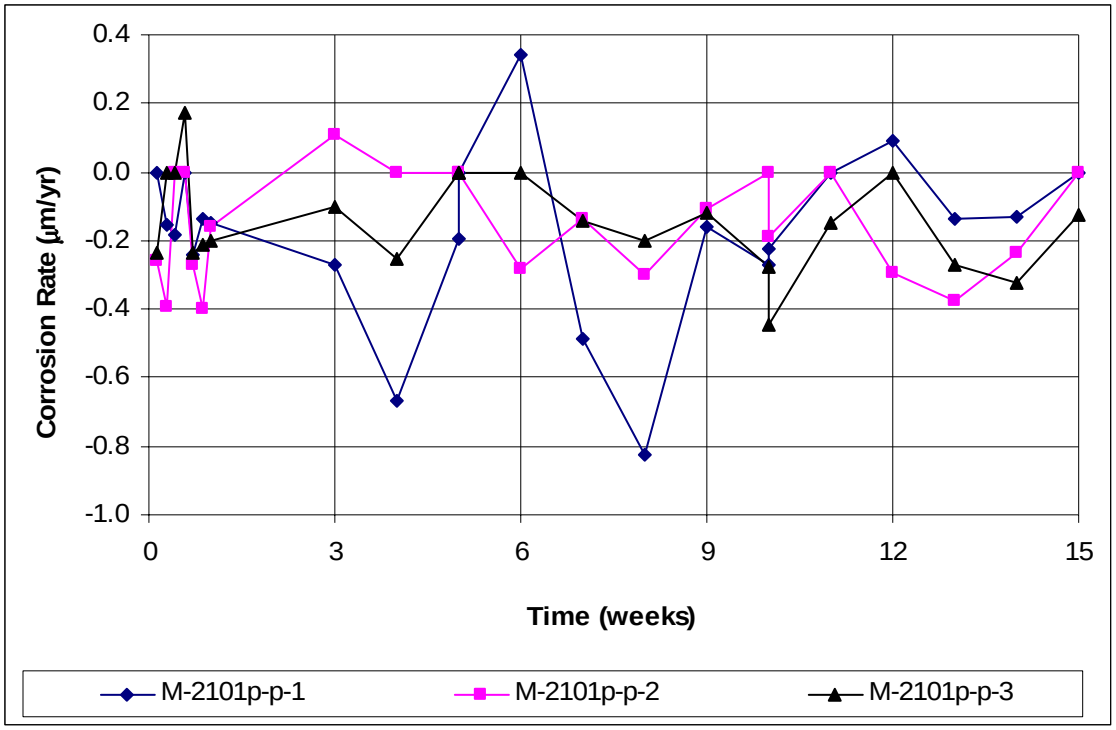

Figure 9: Individual corrosion rate. LDX 2101® specimens 1-3, submerged in simulated pore solution prior to testing.

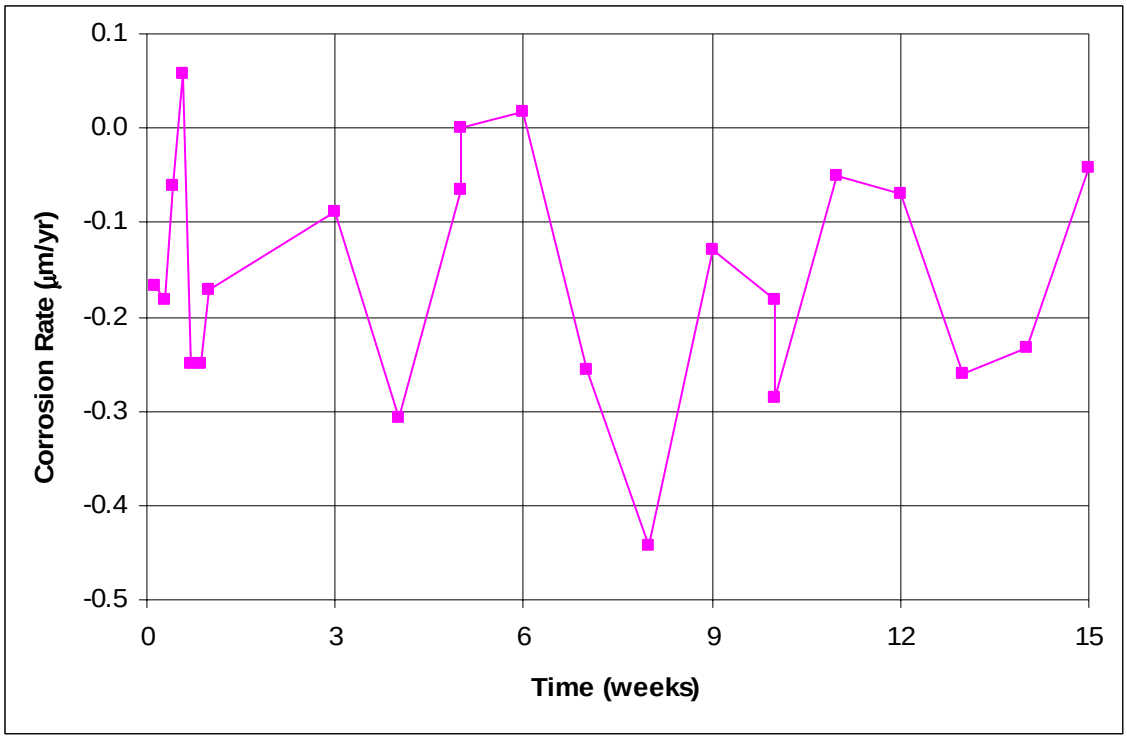

Figure 10: Average corrosion rate. LDX 2101® specimens 1-3, submerged in simulated pore solution prior to testing.

Individual corrosion potential data with respect to a saturated calomel electrode are shown in Figures 11 and 12 for the bars submerged in simulated pore solution prior to testing in salt solution and pore solution, respectively. Potentials for bars in the pore solution were on average 20-30 mV more negative than for bars in the salt solution, similar to the bars tested in the as-received condition.

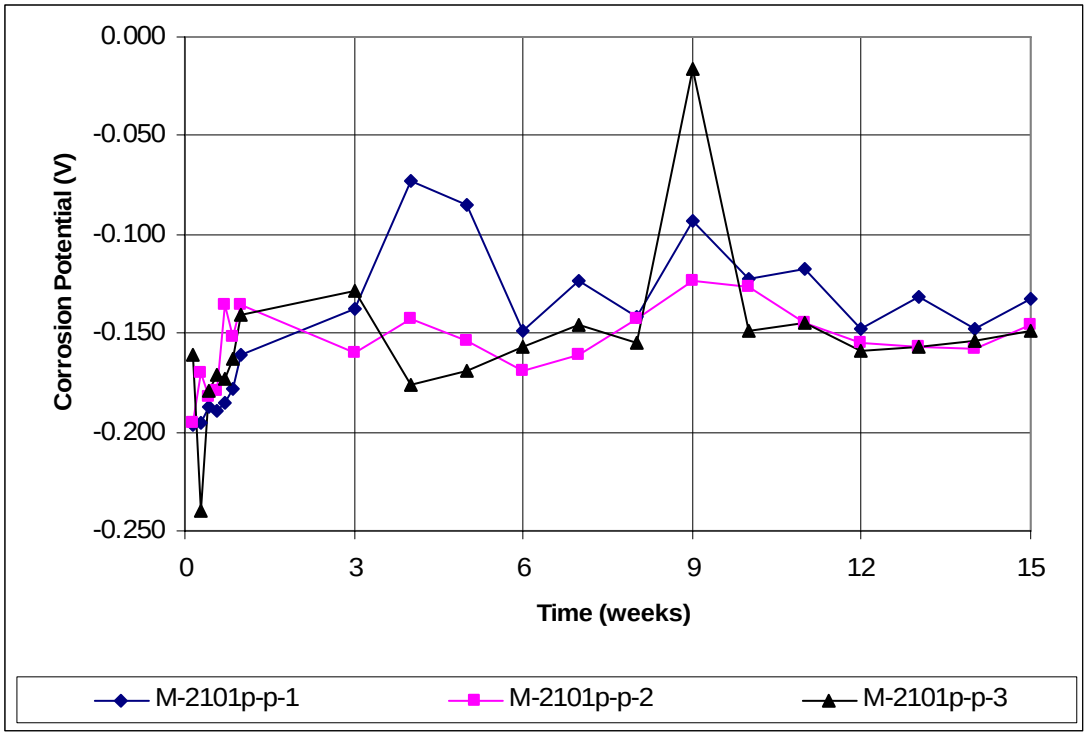

Figure 11: Individual corrosion potential with respect to SCE. Bars in salt solution (anode). LDX 2101® specimens 1-3 submerged in simulated pore solution prior to testing.

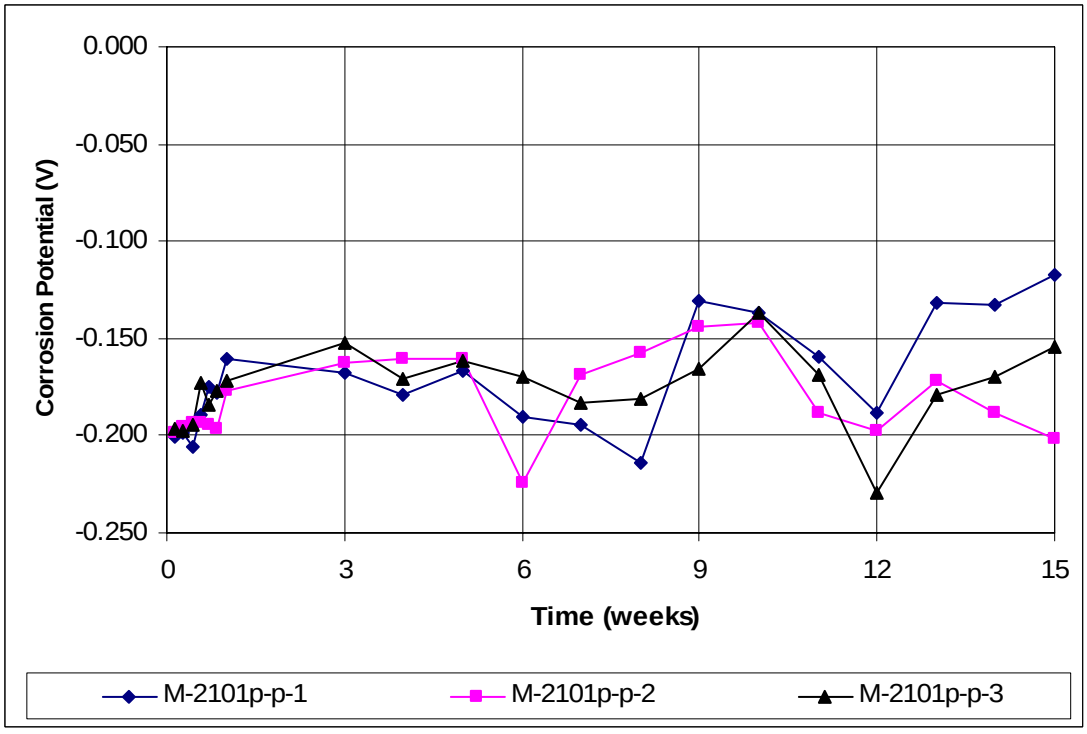

Figure 12: Individual corrosion potential with respect to SCE. Bars in pore solution (cathode). LDX 2101® specimens 1-3, submerged in simulated pore solution prior to testing.

Individual and average corrosion rate data for the 2205 pickled stainless steel specimens are shown in Figures 13 and 14, respectively. As shown in Figures 13 and 14, the 2205p stainless steel specimens exhibited "negative" corrosion similar to LDX 2101® steel, but to a lesser degree. Individual corrosion rates ranged from −0.50 µm/yr to 0.0 µm/yr. At no point was a measurable positive corrosion rate observed for the 2205 stainless steel specimens. Average corrosion rate data are shown in Figure 14. The average corrosion rate varied from -0.21 µm/yr to 0.0 µm/yr, meeting all requirements of Annex A2 of ASTM A955-09b.

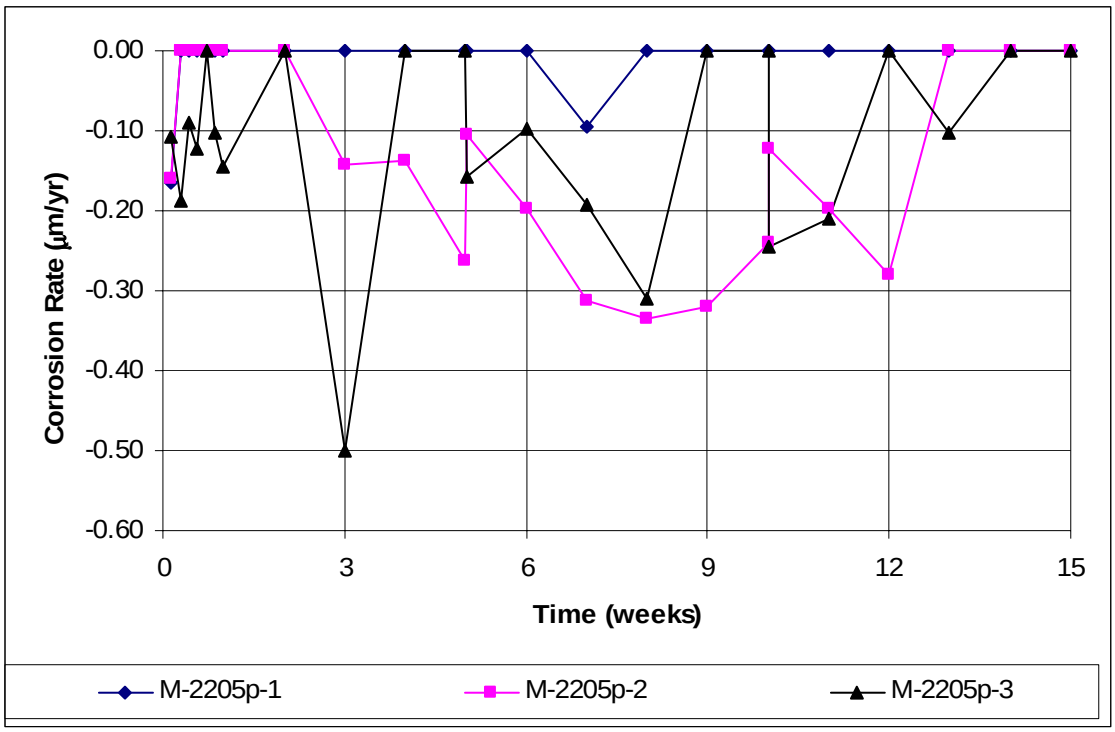

Figure 13: Individual corrosion rate. 2205 specimens 1-3.

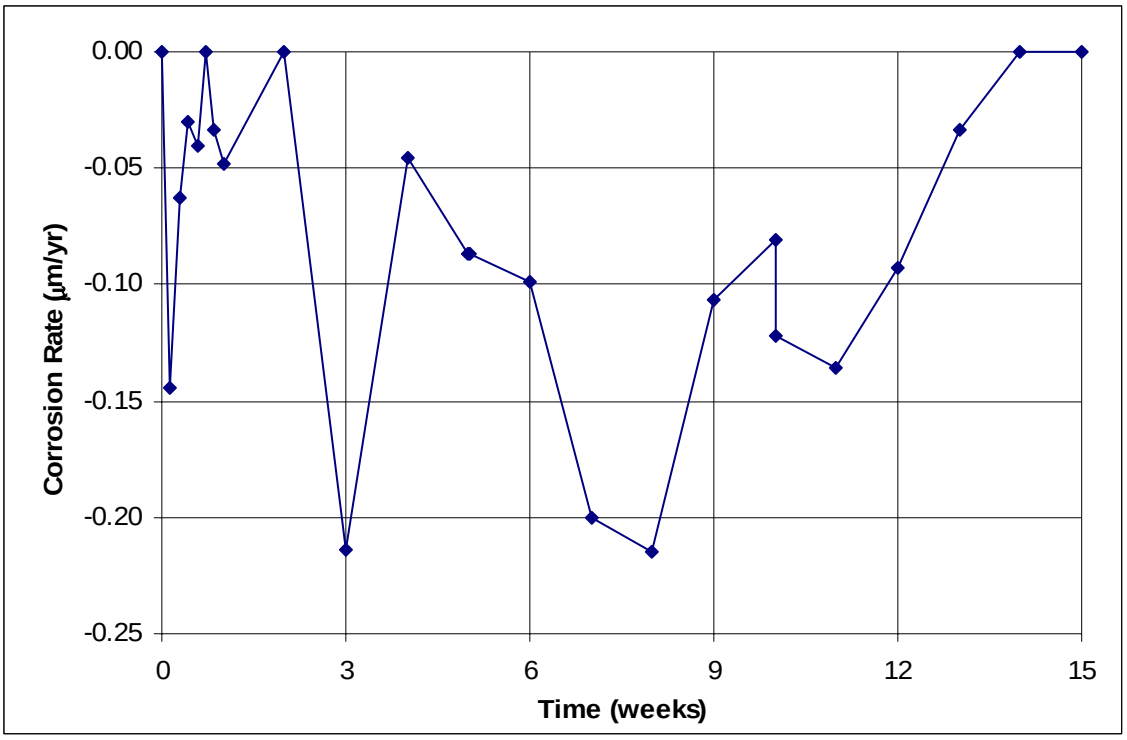

Figure 14: Average corrosion rate. 2205 specimens 1-3.

Individual corrosion potential data with respect to a saturated calomel electrode are shown in Figures 15 and 16 for the 2205p bars in the salt and pore solutions, respectively. Potentials for bars in pore solution, however, were on average 40 mV more negative than bars in salt solution, similar to observed potentials for specimens with LDX 2101® stainless steel. Corrosion potentials at the bars in pore solution for the 2205p stainless steel specimens were slightly more negative than those observed for LDX 2101® stainless steel. However, corrosion rates for 2205p specimens were lower than those of LDX 2101® specimens (compare Figures 6 and 14).

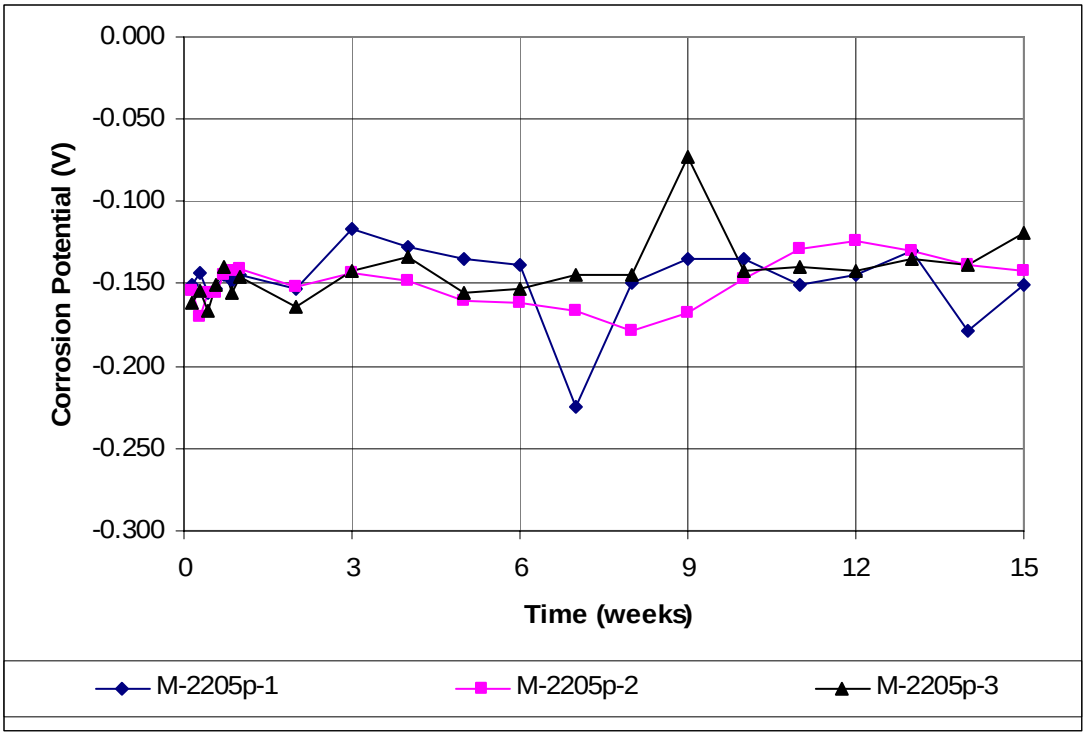

Figure 15: Individual corrosion potential with respect to SCE. Bars in salt solution (anode). 2205p specimens 1-3.

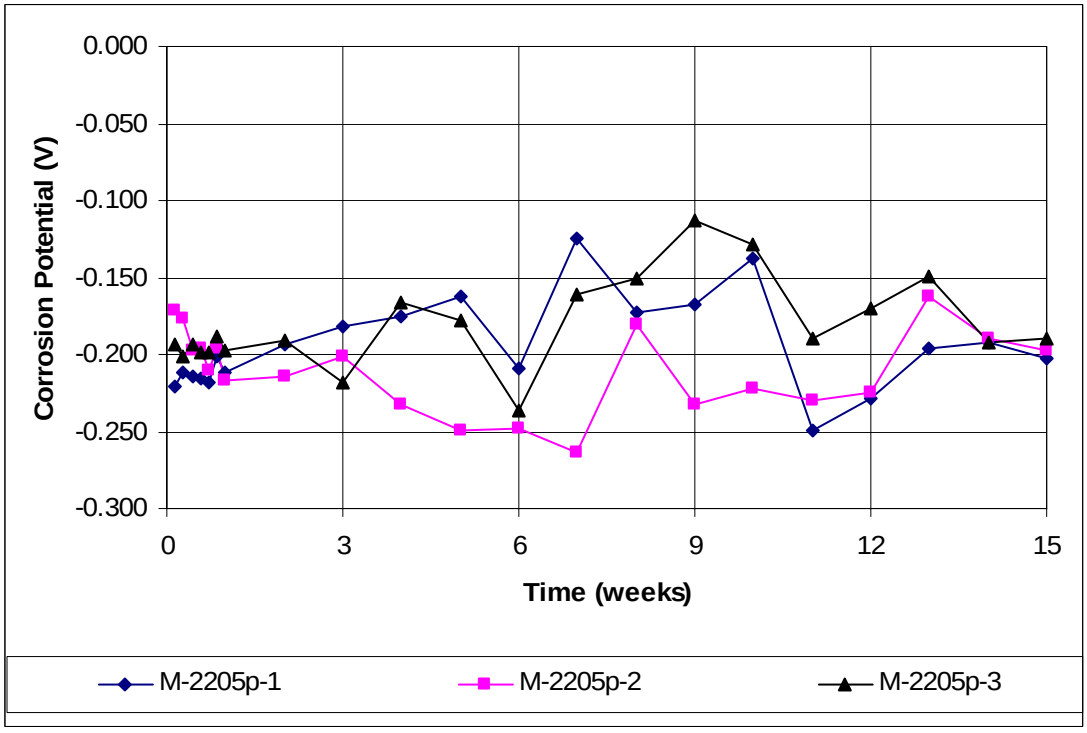

Figure 16: Individual corrosion potential with respect to SCE. Bars in pore solution (cathode). 2205 specimens 1-3.

After testing, specimens were inspected for signs of corrosion. For the nine specimens tested in the as received condition, all specimens showed significant staining on the cathode bars (Figure 17). Furthermore, 7 of the 9 specimens showed limited corrosion products on the anode (Figure 18). Photos of all specimens appear in Appendix A.

Figure 17: LDX 2101® specimen 3, as received condition. Bars at end of test showing staining.

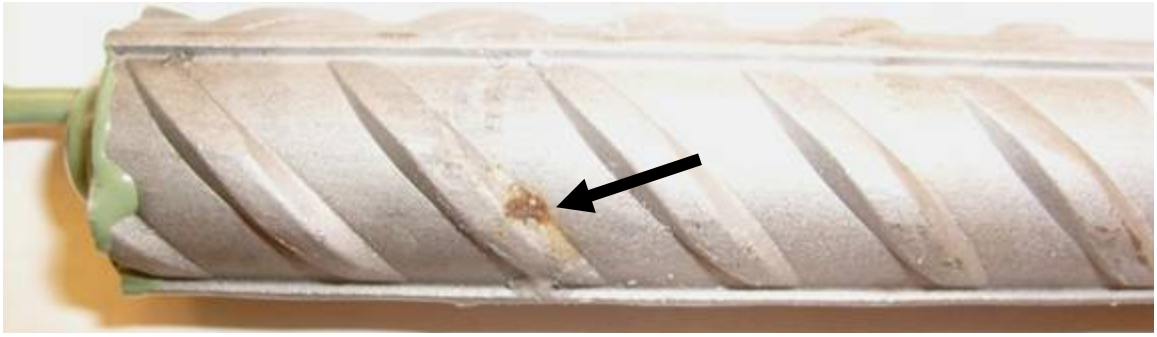

Figure 18: LDX 2101® specimen 6, as received condition. Anode bar at end of test. Limited staining on bar in salt solution.

Of the three LDX 2101® specimens submerged in simulated pore solution prior to testing, one specimen showed moderate staining on the anode (Figure 19), one specimen showed limited staining on the anode (Figure 20), and one specimen showed no staining on the anode. All specimens exhibited moderate staining on the cathode bars.

Figure 19: LDX 2101® specimen 1, submerged in simulated pore solution prior to testing. Bars at end of test showing staining.

Figure 20: LDX 2101® specimen 2, submerged in simulated pore solution prior to testing. Anode bar at end of test. Limited staining on bar in salt solution.

For the three 2205p specimens, all specimens showed light to moderate staining on the cathode bars (Figure 21). No corrosion products were observed on the bars in salt solution.

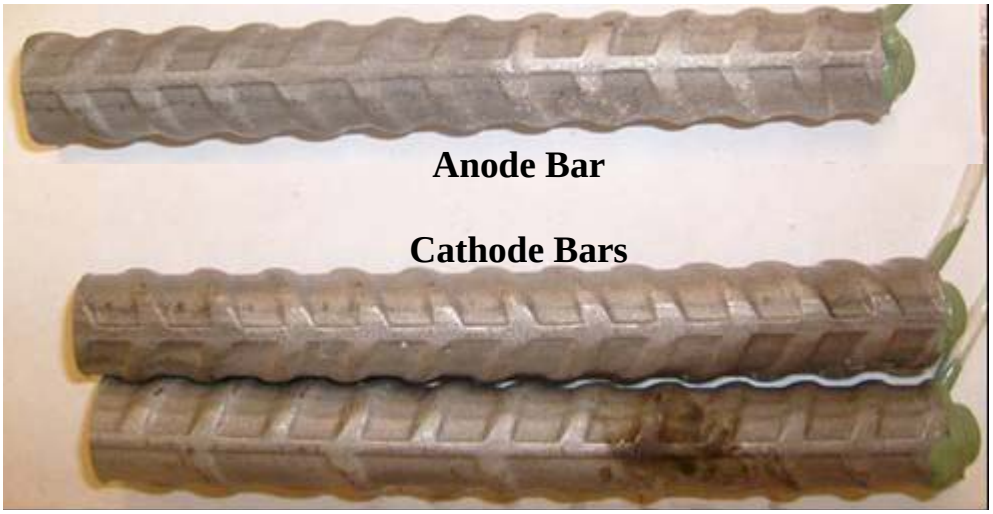

Figure 21: 2205p specimen 3 showing staining at end of test.

SUMMARY AND CONCLUSIONS:

The corrosion resistance of LDX 2101® bars was tested using rapid macrocell tests performed in accordance with Annex A2 of ASTM 955-09b with the exception that No. 6 (No. 19) bars were used in place of No. 5 (No. 16) bars. Comparisons were also made with pickled 2205 stainless steel.

The following conclusions are based on the test results presented in this report:

1. The corrosion resistance of LDX 2101® stainless steel meets the requirements of ASTM A955-09b.
2. The corrosion resistance of the 2205p stainless steel bars exceeds that of LDX 2101® bars when tested in accordance with ASTM A955-09b.
3. Staining on bars in pore solution was observed on all specimens but is not indicative of a susceptibility to chloride-induced corrosion in concrete.

REFERENCES

ACI Committee 408, 2007, "Splice and Development Length of High Relative Rib Area Reinforcing Bars in Tension (ACI 408.3-01)," American Concrete Institute, Farmington Hills, MI.

ASTM A955, 2009, "Standard Specification for Plain and Deformed Stainless-Steel Bars for Concrete Reinforcement (ASTM A955/A955M – 09b)," ASTM International, West Conshohocken, PA, 11 pp.

ASTM C876, 2009, "Standard Test Method for Corrosion Potentials of Uncoated Reinforcing Steel in Concrete (ASTM C876-09)," ASTM International, West Conshohocken PA, 7 pp.

Choi, Oan Chul, Hadje-Ghaffari. Hossain, Darwin, David and McCabe, Steven L., 1990, "Bond of Epoxy-Coated Reinforcement to Concrete: Bar Parameters," *SL Report* 90-1, University of Kansas Center for Research, Lawrence, 43 pp.

Darwin, D. and Graham, E. K., 1993, "Effect of Deformation Height and Spacing on Bond Strength of Reinforcing Bars," *ACI Structural Journal*, Vol. 90, No. 6, Nov.-Dec., pp. 646-657.

APPENDIX A: END OF TEST SPECIMEN PHOTOS

Figure A1: LDX 2101® specimen 1, as received condition. Side A.

Figure A2: LDX 2101® specimen 1, as received condition. Side B.

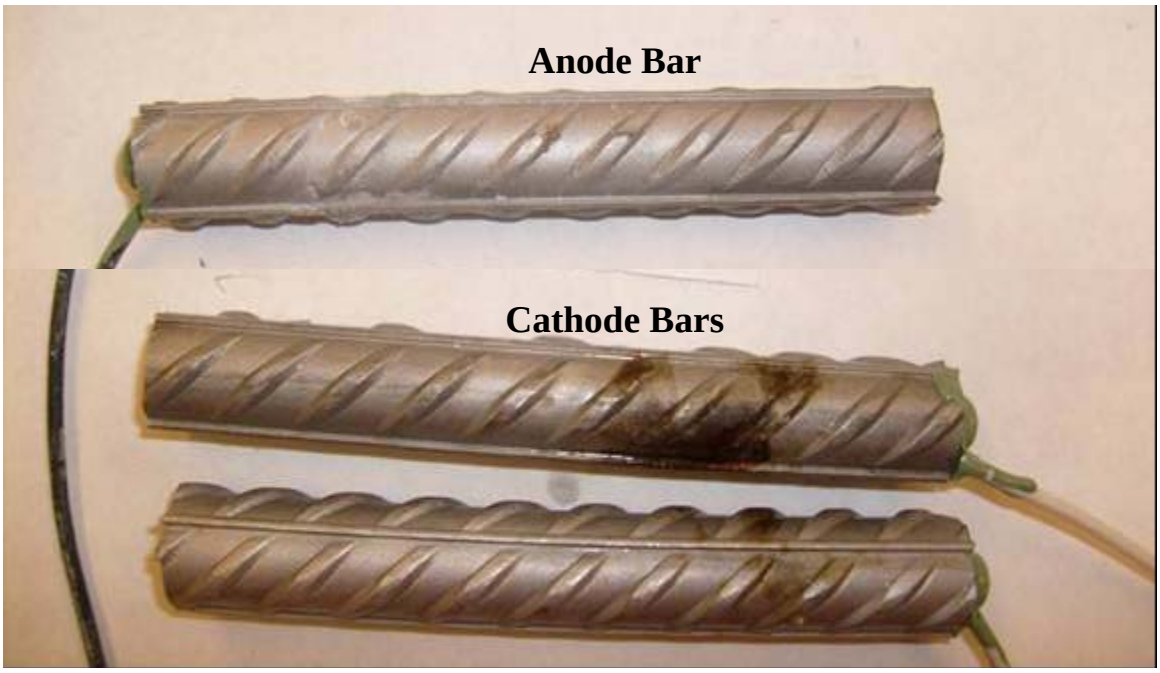

Figure A3: LDX 2101® specimen 2, as received condition. Side A.

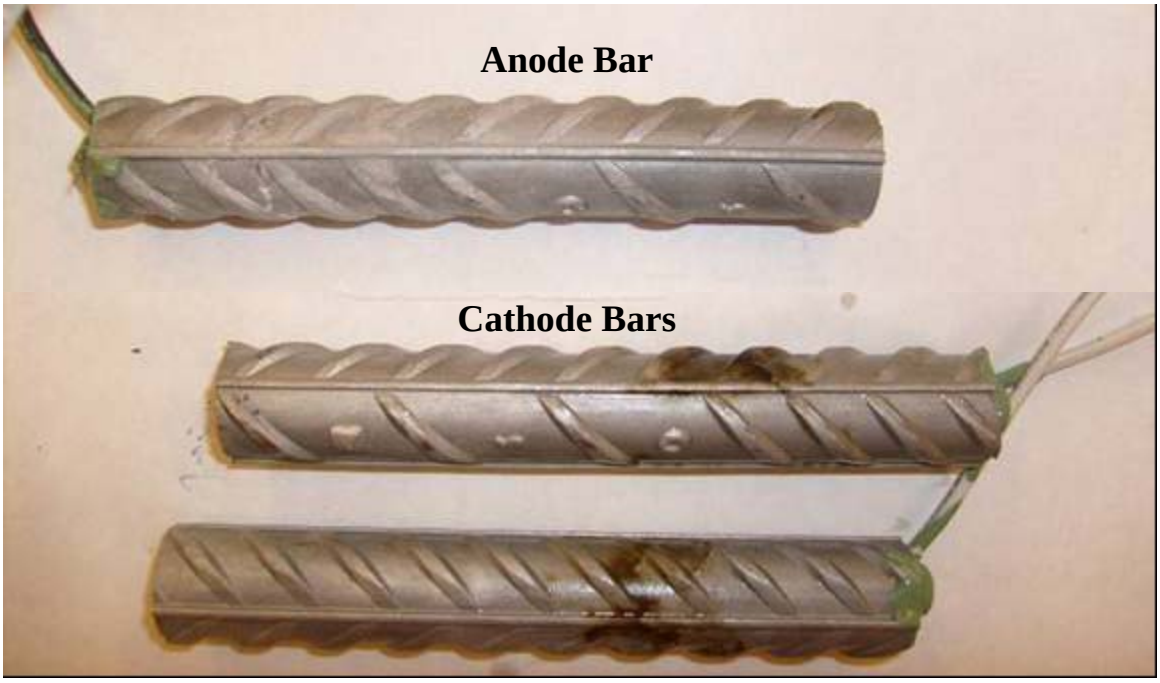

Figure A4: LDX 2101® specimen 2, as received condition. Side B

Figure A5: LDX 2101® specimen 3, as received condition. Side A.

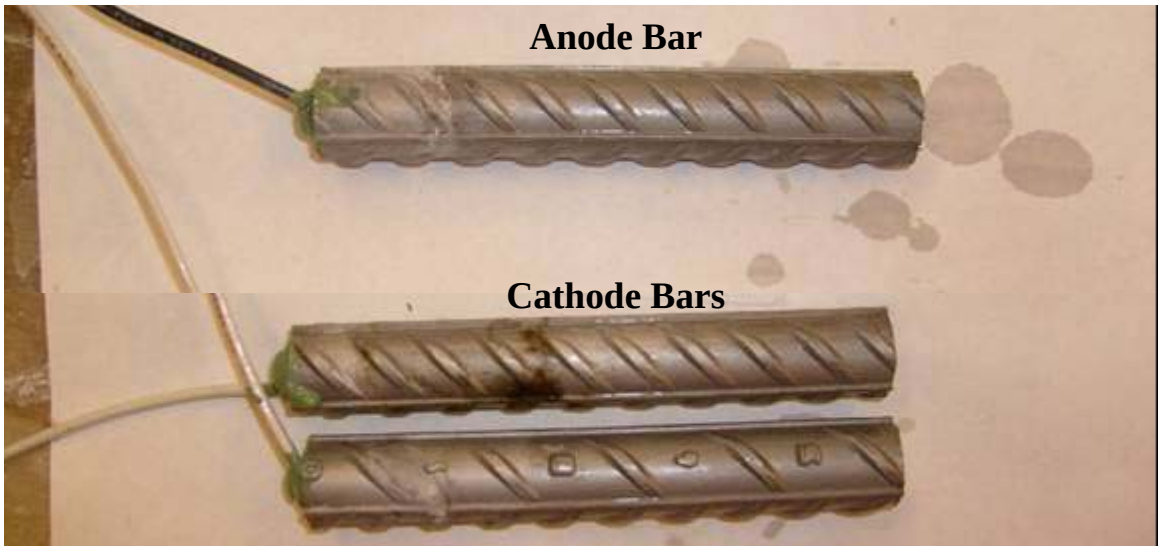

Figure A6: LDX 2101® specimen 3, as received condition. Side B.

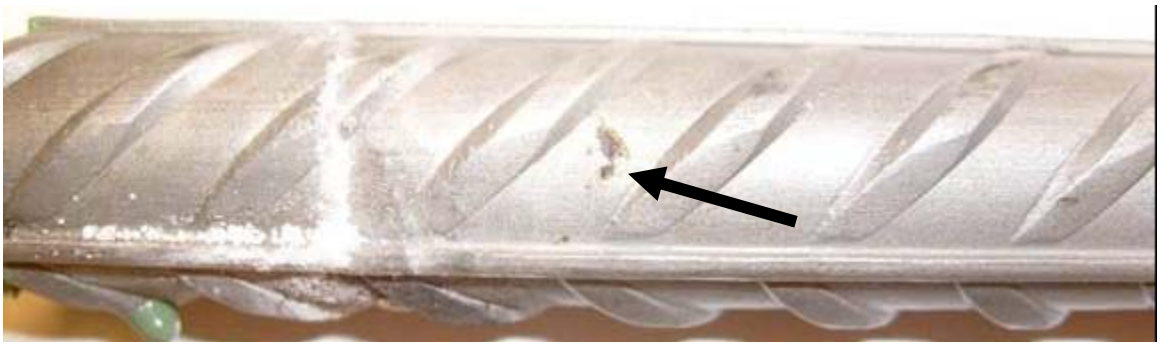

Figure A7: LDX 2101® specimen 3, as received condition. Anode bar.

Figure A8: LDX 2101® specimen 4, as received condition. Side A.

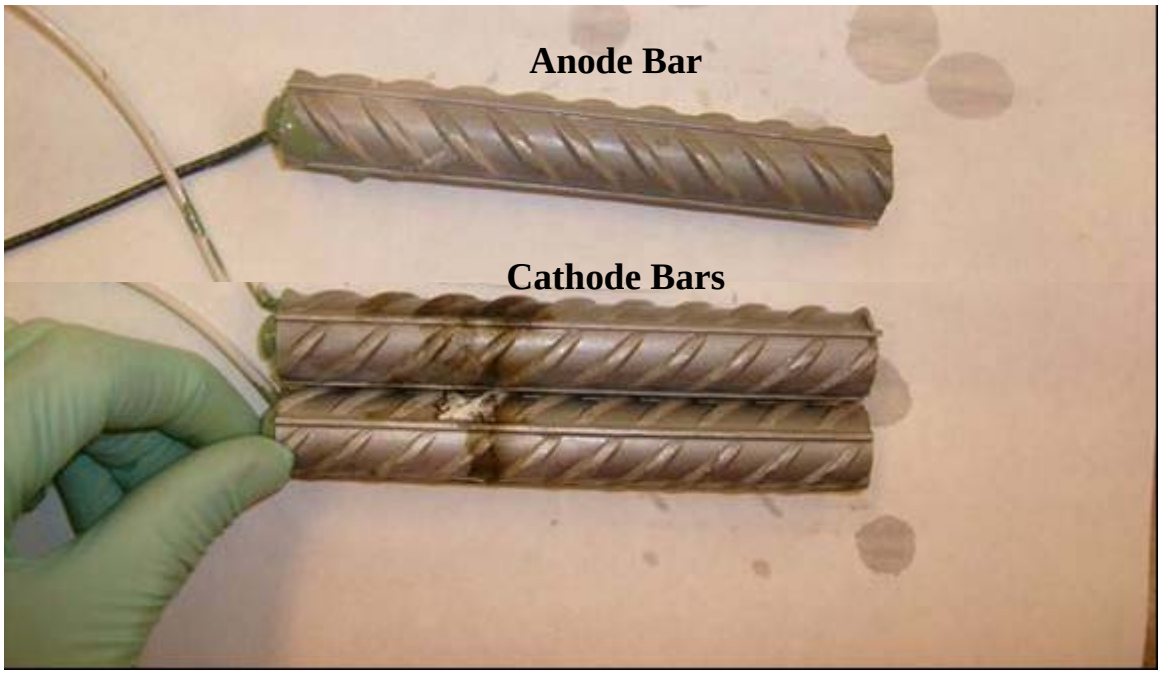

Figure A9: LDX 2101® specimen 4, as received condition. Side B.

Figure A10: LDX 2101® specimen 5, as received condition. Side A.

Figure A11: LDX 2101® specimen 5, as received condition. Side B.

Figure A12: LDX 2101® specimen 6, as received condition. Side A.

Figure A13: LDX 2101® specimen 6, as received condition. Side B.

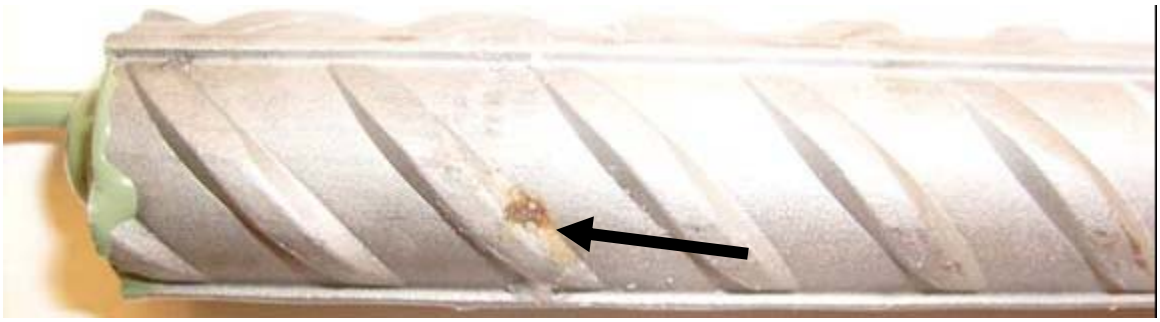

Figure A14: LDX 2101® specimen 6, as received condition. Anode bar.

Figure A15: LDX 2101® specimen 7, as received condition. Side A.

Figure A16: LDX 2101® specimen 7, as received condition. Side B.

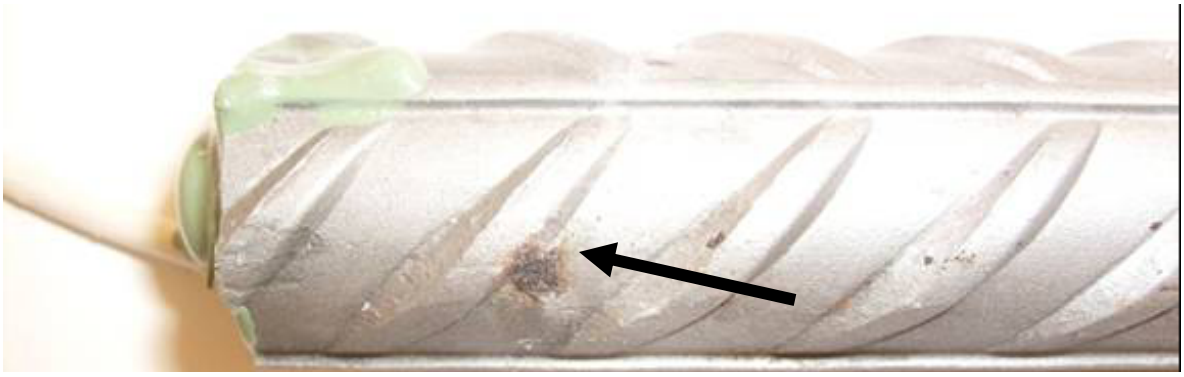

Figure A17: LDX 2101® specimen 7, as received condition. Anode bar.

Figure A18: LDX 2101® specimen 8, as received condition. Side A.

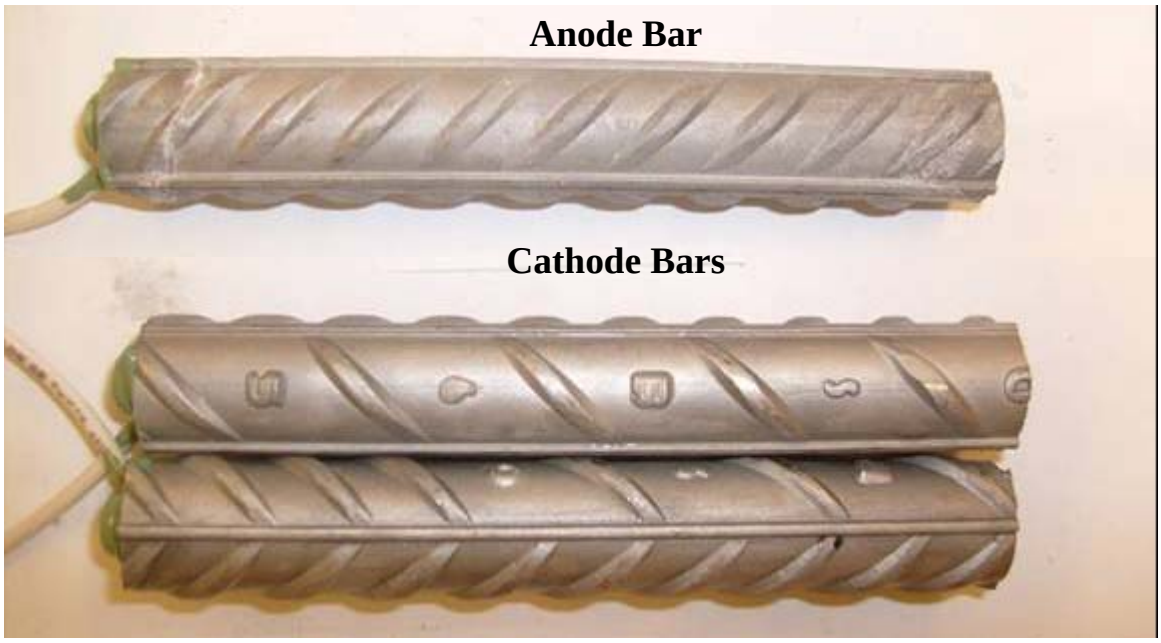

Figure A19: LDX 2101® specimen 8, as received condition. Side B.

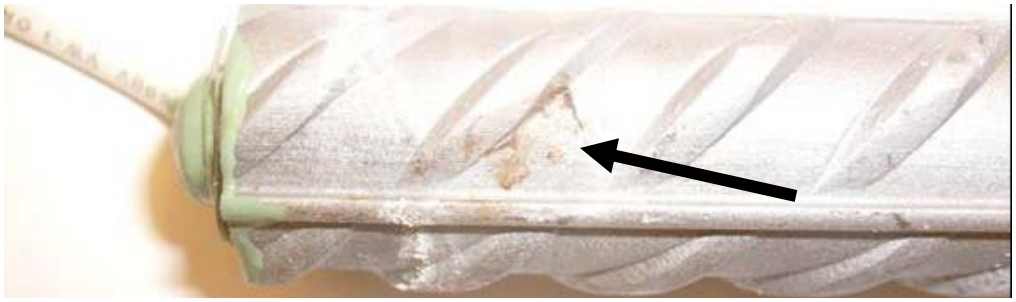

Figure A20: LDX 2101® specimen 8, as received condition. Anode bar.

Figure A21: LDX 2101® specimen 9, as received condition. Side A.

Figure A22: LDX 2101® specimen 9, as received condition. Side B.

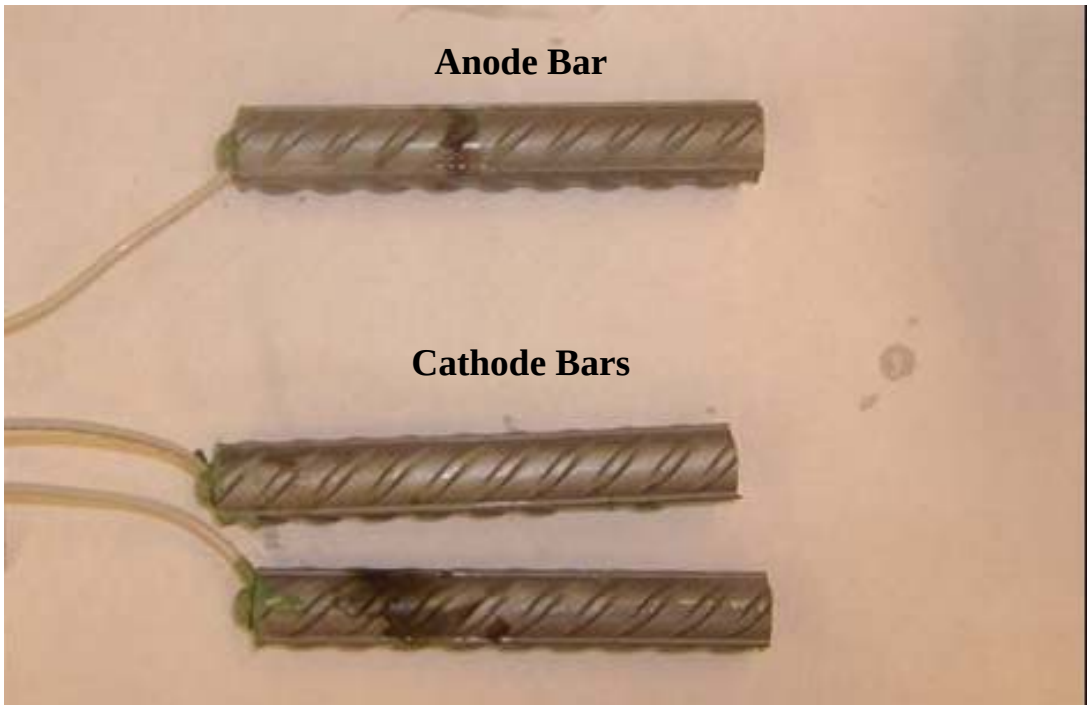

Figure A23: LDX 2101® specimen 1, submerged in simulated pore solution prior to testing. Side A.

Figure A24: LDX 2101® specimen 1, submerged in simulated pore solution prior to testing. Side B.

Figure A25: LDX 2101® specimen 2, submerged in simulated pore solution prior to testing. Side A.

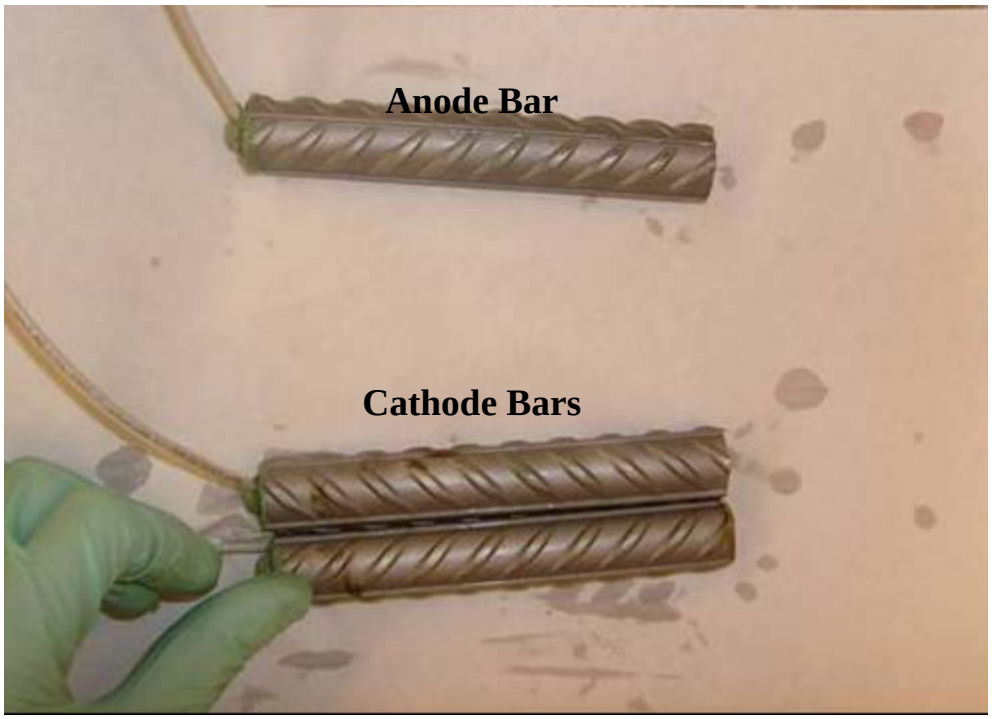

Figure A26: LDX 2101® specimen 2, submerged in simulated pore solution prior to testing. Side B.

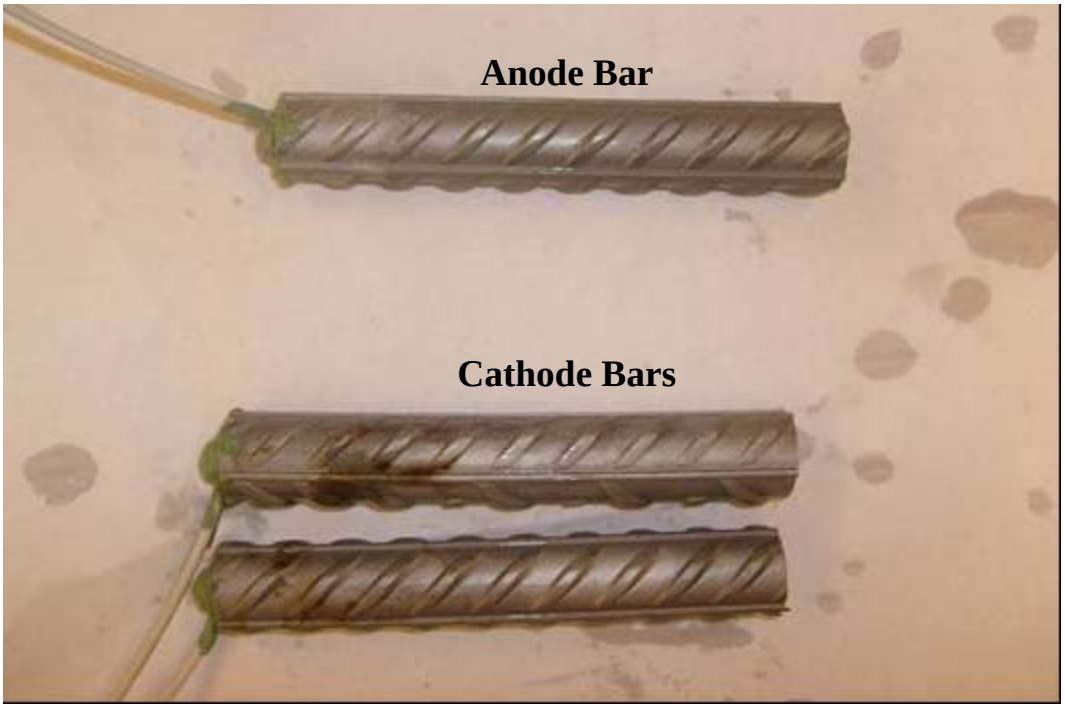

Figure A27: LDX 2101® specimen 3, submerged in simulated pore solution prior to testing. Side A.

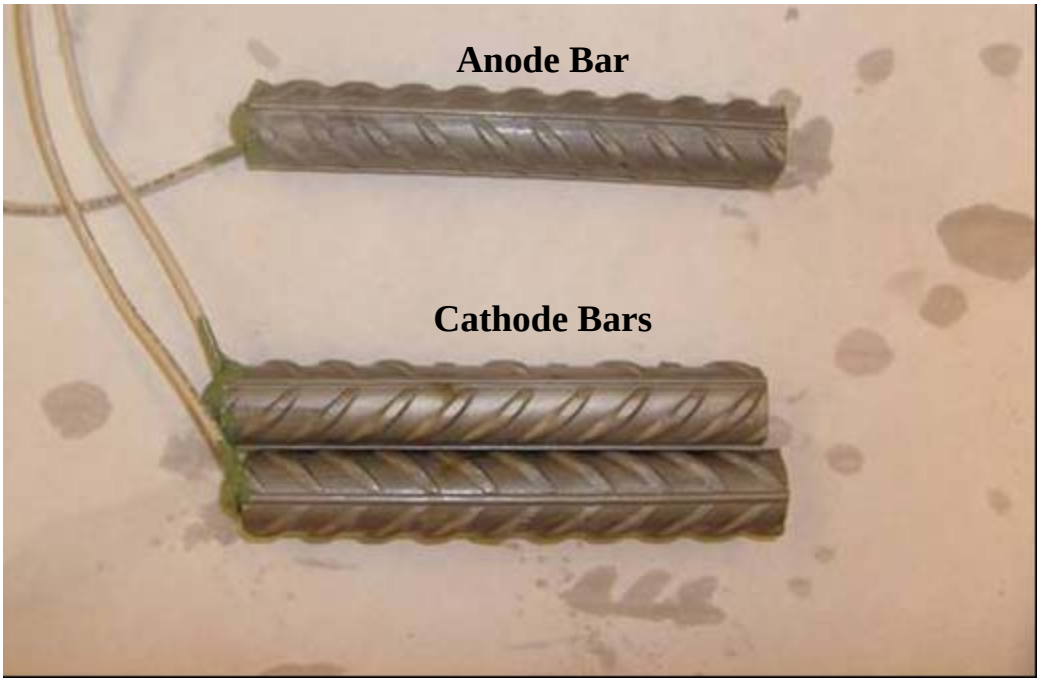

Figure A28: LDX 2101® specimen 3, submerged in simulated pore solution prior to testing. Side B.

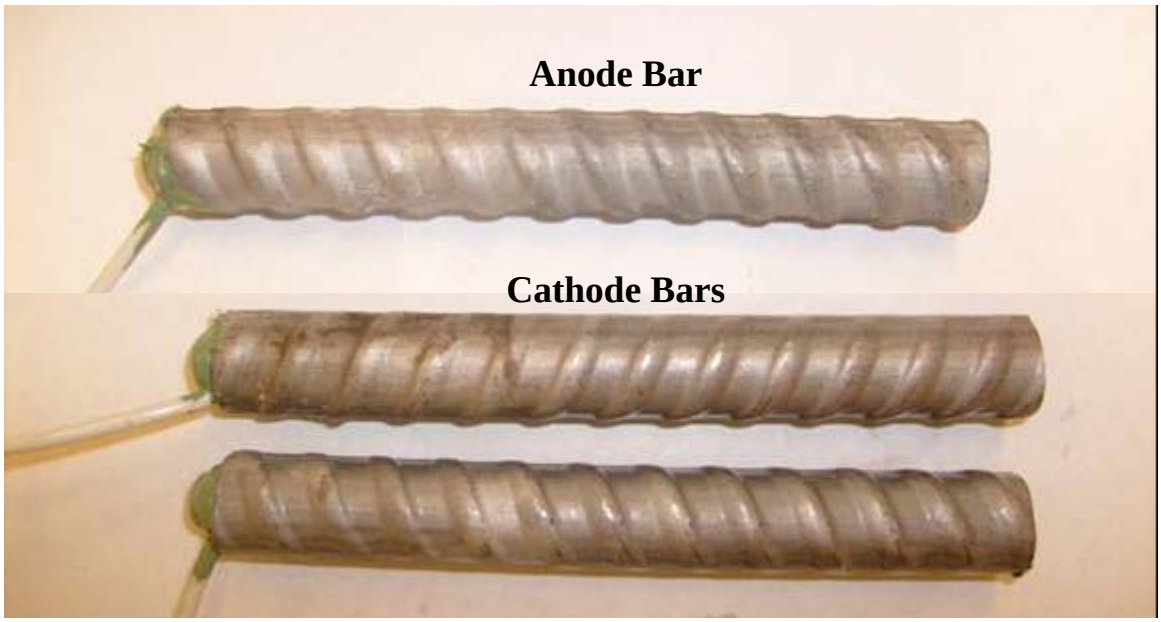

Figure A29: 2205p specimen 1. Side A.

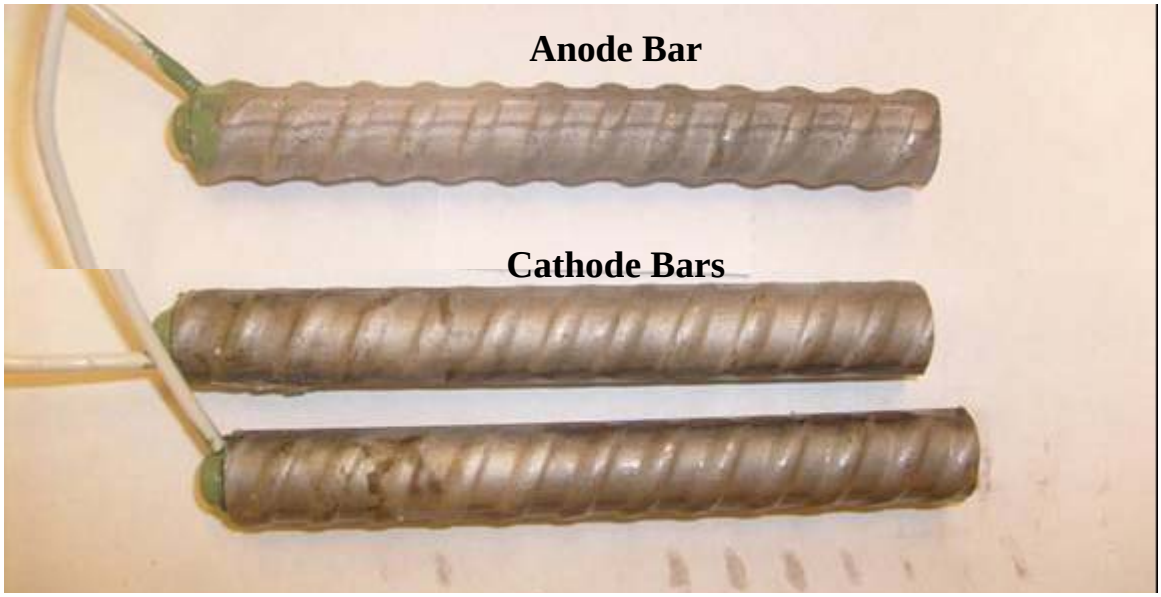

Figure A30: 2205p specimen 1. Side B.

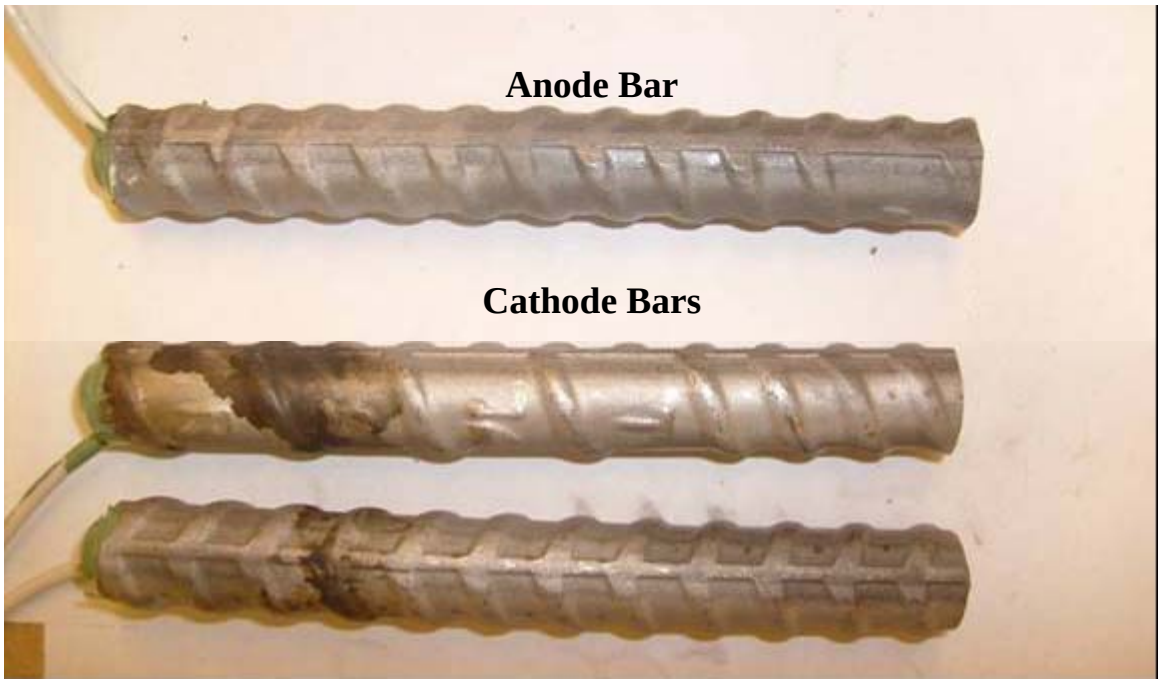

Figure A31: 2205p specimen 2. Side A.

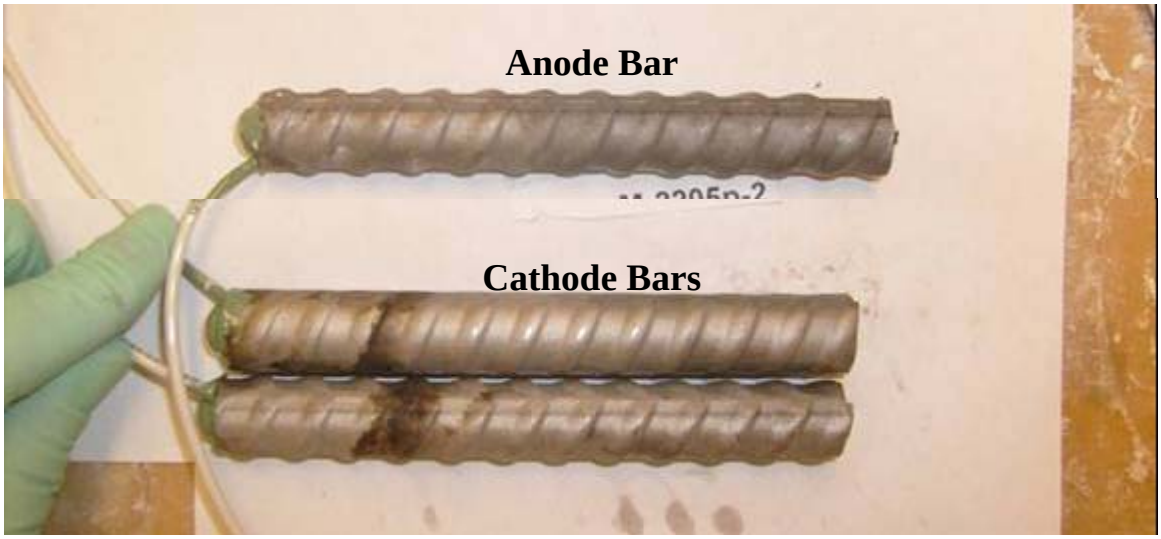

Figure A32: 2205p specimen 2. Side B.

Figure A33: 2205p specimen 3. Side A.

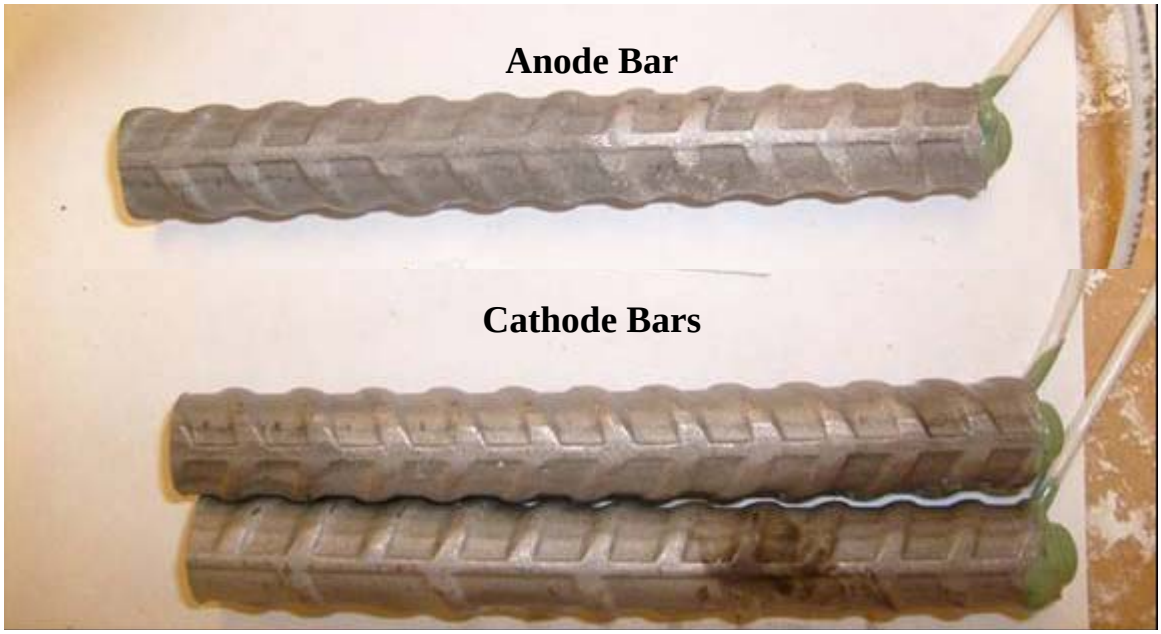

Figure A33: 2205p specimen 3. Side B.